NASA CONTRACTOR REPORT






# CALCULATION OF LAMINAR AND TURBULENT BOUNDARY LAYERS FOR TWO-DIMENSIONAL TIME-DEPENDENT FLOWS

*Tuncer Cebeci*

*Prepared by*
CALIFORNIA STATE UNIVERSITY AT LONG BEACH
Long Beach, Calif.
*for Langley Research Center*

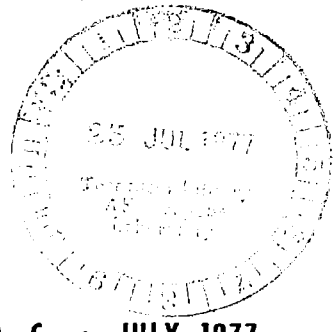


NATIONAL AERONAUTICS AND SPACE ADMINISTRATION • WASHINGTON, D. C. • JULY 1977

| 1. Report No. | 2. Government Accession No. | 3. Recipient's Catalog No. |
|---|---|---|
| NASA CR-2820 | | |

| 4. Title and Subtitle | 5. Report Date |
|---|---|
| Calculation of Laminar and Turbulent Boundary Layers for Two-Dimensional Time-Dependent Flows | June 1977 |
| | 6. Performing Organization Code 36.320 |
| 7. Author(s) Tuncer Cebeci | 8. Performing Organization Report No. |
| | 10. Work Unit No. |
| 9. Performing Organization Name and Address California State University at Long Beach Long Beach, California | 11. Contract or Grant No. NAS1-13656 |
| | 13. Type of Report and Period Covered Contractor Report |
| 12. Sponsoring Agency Name and Address National Aeronautics and Space Administration Washington, DC 20546 | 14. Sponsoring Agency Code |

15. Supplementary Notes

Final report.- The contract research effort was carried out in cooperation with Dr. Lawrence W. Carr, U.S. Army Air Mobility R&D Laboratory - Ames Directorate. Langley technical monitor: Warren H. Young, Jr.

16. Abstract

A general method for computing laminar and turbulent boundary layers for two-dimensional time-dependent flows is presented. The method uses an eddy-viscosity formulation to model the Reynolds shear-stress term and a very efficient numerical method to solve the governing equations. The model has previously been applied to steady two-dimensional and three-dimensional flows and has been shown to give good results.

A discussion of the numerical method and the results obtained by the present method for both laminar and turbulent flows are discussed. Based on these results, the method is efficient and suitable for solving time-dependent laminar and turbulent boundary layers.

| 17. Key Words (Suggested by Author(s)) | 18. Distribution Statement |
|---|---|
| Boundary layer, dynamic stall, unsteady boundary layer, turbulent boundary layer | Unclassified - Unlimited<br>Subject Category 34 |

| 19. Security Classif. (of this report) | 20. Security Classif. (of this page) | 21. No. of Pages | 22. Price* |
|---|---|---|---|
| Unclassified | Unclassified | 35 | $4.00 |

* For sale by the National Technical Information Service, Springfield, Virginia 22161

TABLE OF CONTENTS

## LIST OF SYMBOLS

| | |
|---|---|
| $A$ | Van Driest damping parameter |
| $B$ | amplitude |
| $c_f$ | local skin-friction coefficient |
| $f$ | dimensionless stream function |
| $K$ | variable grid parameter |
| $P, P_3$ | pressure-gradient parameters, see (24) |
| $p$ | pressure |
| $P_x^+, P_t^+$ | dimensionless-pressure-gradient parameters |
| $R_x$ | Reynolds number based on $x$, $u_0 x/\nu$ |
| $R_{\delta^*}$ | Reynolds number based on displacement thickness, $u_0 \delta^*/\nu$ |
| $R_\theta$ | Reynolds number based on momentum thickness, $u_0 \theta/\nu$ |
| $u, v$ | velocity components in the $x$ and $y$ directions, respectively |
| $u_\tau$ | friction velocity |
| $x, y$ | Cartesian coordinates |
| $y^+$ | Cartesian dimensionless distance, $yu_\tau/\nu$ |
| $\alpha$ | parameter in the outer eddy-viscosity formula |
| $\delta$ | boundary-layer thickness |
| $\delta^*$ | displacement thickness |
| $\varepsilon_m$ | eddy viscosity |
| $\eta$ | similarity variable for $y$ |
| $\eta_\infty$ | transformed boundary-layer thickness |
| $\theta$ | momentum thickness |
| $\mu$ | dynamic viscosity |
| $\nu$ | kinematic viscodity |
| $\rho$ | density |
| $\omega$ | angular velocity, rad/sec |
| $\tau$ | shear stress |

$\psi$ stream function

$\phi$ phase angle

Subscripts

e edge

o steady state

w wall

Primes denote differentiation with respect to $\eta$

# CALCULATION OF LAMINAR AND TURBULENT BOUNDARY LAYERS FOR TWO-DIMENSIONAL TIME-DEPENDENT FLOWS

by

Tuncer Cebeci

## I. SUMMARY

In recent years several methods have been developed to compute time-dependent laminar and turbulent boundary layers. Some of these methods use the eddy-viscosity, mixing-length concepts to model the Reynolds stresses (for example, see references 1 and 2), and others use the approach advocated by Bradshaw (see for example, references 3 and 4). The chief advocates of Bradshaw's method are Nash and Patel.

A general method for computing laminar and turbulent boundary layers for two-dimensional time-dependent flows is presented in this report. The method uses an eddy-viscosity formulation to model the Reynolds shear-stress term and a very efficient numerical method to solve the governing equations. The model developed by Cebeci, has been applied to two-dimensional flows[5] and to three-dimensional flows[6,7] and has been shown to give good results.

In Section II the governing equations and the eddy-viscosity formulas are presented. When physical coordinates are used, the numerical solutions of the boundary-layer equations are quite sensitive to the spacings in the x- and t-directions. In problems where computation time and storage become important, it is desirable to reduce the sensitivity to $\Delta t$- and $\Delta x$-spacings. This can be done by expressing and by solving the governing equations in appropriate transformed coordinates and transformed variables. In Section II we introduce such transformations.

Section III presents a discussion of the numerical method and in Section IV the results obtained by the present method for both laminar and turbulent flows are discussed. Based on the results given in this report, we find the method quite efficient and suitable for solving time-dependent flows for both laminar and turbulent boundary layers.

## II. GOVERNING EQUATIONS

### 2.1 Boundary-Layer Equations

The continuity and momentum equations for incompressible, unsteady laminar and turbulent boundary layers are:

Continuity

$$\frac{\partial u}{\partial x} + \frac{\partial v}{\partial y} = 0 \tag{1}$$

Momentum

$$\frac{\partial u}{\partial t} + u\,\frac{\partial u}{\partial x} + v\,\frac{\partial u}{\partial y} = \frac{\partial u_e}{\partial t} + u_e\,\frac{\partial u_e}{\partial x} + \frac{1}{\rho}\,\frac{\partial}{\partial y}\left[\mu\,\frac{\partial u}{\partial y} - \rho\overline{u'v'}\right] \tag{2}$$

The boundary conditions for the wall and for the outer edge of the boundary layer are:

$$y = 0 \qquad u,\ v = 0 \tag{3a}$$

$$y \to \infty \qquad u \to u_e(x,t) \tag{3b}$$

To complete the formulation of the problem, additional boundary conditions must be specified on some initial upstream surface, $t = T(x)$ say, normal to the x-t-plane. Here we consider the simple case where this surface is made up of the two surfaces $t = t_a = \text{const.}$ and $x = x_a = \text{const.}$ The required boundary conditions are:

$$t = t_a \quad \text{and} \quad x \geq x_a \quad ; \qquad u = u_a(x,y) \tag{4a}$$

$$x = x_a \quad \text{and} \quad t \geq t_a \quad ; \qquad u = u_a(t,y) \tag{4b}$$

Thus at some initial time, conditions are specified everywhere and for subsequent time, conditions are specified on some upstream station.

### 2.2 Closure Assumptions for the Reynolds Shear Stress

The solution of the system given by (1) to (4) requires closure assumptions for the Reynolds shear stress $-\overline{u'v'}$. In our study we use the eddy viscosity concept and define

$$-\rho\overline{u'v'} = \rho\varepsilon_m\,\frac{\partial u}{\partial y} \tag{5}$$

According to the eddy viscosity formulation of ref. 5, the turbulent boundary layer is divided into two regions, called inner and outer regions, and the eddy viscosity is defined by separate formulas in each region. They are:

$$\varepsilon_m = \begin{cases} (\varepsilon_m)_i = \left\{0.4y\,[1 - \exp(-y/A)]\right\}^2 \left|\frac{\partial u}{\partial y}\right| & (\varepsilon_m)_i \le (\varepsilon_m)_o \qquad (6a) \\ (\varepsilon_m)_o = \alpha \int_0^\infty (u_e - u)dy & (\varepsilon_m)_o \ge (\varepsilon_m)_i \qquad (6b) \end{cases}$$

In (6a), A is a damping-length constant. For an incompressible flow with no mass transfer, it is given by

$$A = 26\nu \left(\frac{\tau_s}{\rho}\right)^{-1/2} \qquad (7a)$$

$$\left(\frac{\tau_s}{\rho}\right)^{1/2} = u_\tau (1 - 11.8p_x^+)^{1/2}, \quad p_x^+ = \frac{\nu u_e}{u_\tau^3}\frac{du_e}{dx}, \quad u_\tau = \left(\frac{\tau_w}{\rho}\right)^{1/2} \qquad (7b)$$

The parameters $\alpha$ is an "universal" constant equal to 0.0168 for high Reynolds number flows, $R_\theta > 5000$. At low Reynolds number its variation can be approximated by a formula given by Cebeci

$$\alpha = \alpha_o \frac{1.55}{1 + \Pi} \qquad (8)$$

$$\Pi = 0.55[1 - \exp(-0.243z_1^{1/2} - 0.298z_1)]$$

where $z_1 = (R_\theta/425 - 1)$.

Equation (7a) was proposed by Cebeci[5]. For a flat-plate flow ($p_x^+ = 0$), it reduces to a form proposed by Van Driest[5]. Cebeci's extension was made by following Van Driest's modeling of the viscous sublayer to Stokes flow. The shear-wave propagation velocity in Stokes flow was assumed to be the friction velocity obtained at a $y^+$-value determined by the intersection of the linear law of the wall with the log law of the wall (rather than its wall value as was assumed by Van Driest) that is,

$$(\omega\nu)^{1/2} = \left(\frac{\tau_s}{\rho}\right)^{1/2} \qquad (9)$$

The friction velocity $(\tau_s/\rho)^{1/2}$ at the intersection of the linear law of the wall with the log law was determined from the momentum equation approximated close to the wall by (no mass transfer)

$$\frac{d\tau}{dy} = \frac{dp}{dx} \tag{10}$$

The solution of (10) with $y_s^+ = y_s/\nu\, u_\tau = 11.8$, that is,

$$\frac{\tau_s}{\tau_w} = 1 - 11.8p_x^+ \tag{11}$$

enables the damping-length constant A to be written in the form given by (7a).

Although this type of approach is highly speculative, and may have little theoretical basis (if any), the expression for A obtained in this manner worked well for turbulent boundary layers with heat and mass transfer[5]. As an example, we compare the predictions of this approach for an incompressible flow with no mass transfer. In reference 8, Back, et al, presented some results on the generation of turbulence near a smooth boundary in a variable free-stream velocity flow by using an analysis based on the extension of Einstein and Li's model[9]. According to the predictions of that model, the ratio of the sublayer growth frequency $\omega$ to that of a flat-plate, $\omega_{f.p.}$, varies with $\zeta$ in the manner shown in Figure 1. The parameter $\zeta$ on which the frequency of sublayer growth depends is given by

$$\zeta = 1.21u_s^+p_x^+ \tag{12}$$

where $u_s^+$ is the nondimensional velocity at the edge of the sublayer, $u_s/u_\tau$ and was assumed to be 15.6 in Einstein and Li's analysis as well as in Back's analysis.

According to (9), $\omega$ is given by

$$\omega = \frac{1}{\nu}\left(\frac{\tau_s}{\rho}\right) \tag{13}$$

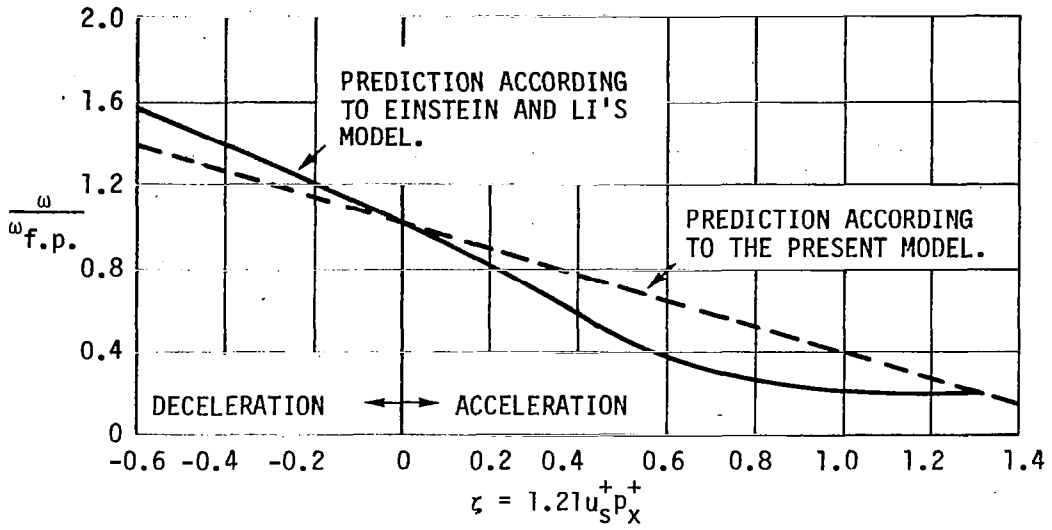


Figure 1. Comparison of predictions of the present model with those of Einstein and Li's model.

We see that with $u_s^+ = 15.6$, equation (11) can also be written as

$$\frac{\omega}{\omega_{f.p.}} = 1 - 0.625\zeta \tag{14}$$

The predictions of (14) with those predicted by the extension of Einstein-Li's model are shown in Figure 1.

Cebeci's extension of Van Driest model to unsteady flows is described in reference 10. For completeness, we include it here. For an incompressible flow with no mass transfer, integration of (10) between the wall and $y_s$, yields

$$\tau_s = \tau_w + \frac{\partial p}{\partial x} y_s \tag{15}$$

Noting that,

$$\frac{\partial p}{\partial x} = \rho\left(u_e \frac{\partial u_e}{\partial x} + \frac{\partial u_e}{\partial t}\right) \tag{16}$$

we can write (15) as

$$\frac{\tau_s}{\tau_w} = 1 - 11.8\ (p_t^+ + p_x^+) \tag{17}$$

Here $p_x^+$ is given by the second expression in (7b) and $p_t^+$ is defined by

$$p_t^+ = \frac{\nu}{u_e^3}\frac{\partial u_e}{\partial t} \tag{18}$$

Thus (7a) becomes

$$A = 26\nu u_\tau^{-1}\ [1 - 11.8(p_t^+ + p_x^+)]^{-1/2} \tag{19}$$

## 2.3 Transformation of the Governing Equations

The boundary-layer equations (1) to (2) subject to (3) and (4) can be solved when they are expressed either in physical coordinates or in transformed coordinates. Each coordinate has its own advantages. In problems where the computer storage becomes important, the choice of using transformed coordinates becomes necessary, as well as convenient, since the transformed coordinates allow large steps to be taken in the x- and t-directions. The reason is that the profiles expressed in the transformed coordinates do not change as rapidly as they do when they are expressed in physical coordinates. The use of transformed coordinates stretches the coordinate normal to the flow and takes out much of the variation in boundary-layer thickness for laminar flows. In addition, they remove the singularity that the equations in physical coordinates have at $x = 0$ for all time.

We first use the transformed coordinate $\eta$ defined by

$$\eta = \sqrt{\frac{u_0(x)}{\nu x}}\, y \tag{20}$$

and introduce a dimensionless stream function $f(x, t, \eta)$ defined in

$$\psi = \sqrt{\nu x u_0}\ f(x,t,\eta) \tag{21}$$

Here $u_o(x)$ is some reference velocity and

$$u = \frac{\partial \psi}{\partial y} \quad , \qquad v = -\frac{\partial \psi}{\partial x} \tag{22}$$

With the relations defined by (20) to (22) and with the definition of eddy viscosity, (5), it can be shown that the momentum equation can be written as

$$(bf'')' + \frac{P+1}{2} ff'' - P(f')^2 + P_3 = x\left(f' \frac{\partial f'}{\partial x} - f'' \frac{\partial f}{\partial x} + \frac{1}{u_o} \frac{\partial f'}{\partial t}\right) \tag{23}$$

Here primes denote differentiation with respect to $\eta$ and

$$f' = \frac{u}{u_o} \quad , \quad P = \frac{x}{u_o} \frac{du_e}{dx} \quad , \quad P_3 = \frac{x}{u_o^2} \left(u_e \frac{\partial u_e}{\partial x} + \frac{\partial u_e}{\partial t}\right) \quad , \quad b = 1 + \epsilon_m^+ \tag{24}$$

The boundary conditions given by (3) become

$$\eta = 0 \qquad f = f' = 0 \tag{25a}$$

$$\eta \to \eta_\infty \qquad f' = u_e/u_o \tag{25b}$$

Similarly the initial conditions given by (4) can be transformed. For some problems where the flow starts as laminar, they can be obtained from (23). Along the $\eta$-$t$ plane where $x = 0$, (23) reduces to

$$f''' + \frac{P+1}{2} ff'' - P(f')^2 + P_3 = \frac{x}{u_o} \frac{\partial f'}{\partial t} \tag{26}$$

Note that, in general, the right-hand side of (26) is not equal to zero. For example, although for a flat-plate flow it is equal to zero, for stagnation-point flow ($u_o = Ax$), it is not. For generality we will keep it in that form.

The specification of the initial conditions at $t = t_a$ and $x \geq x_a$ requires special treatment. Here for simplicity we assume that they are given by the steady-state conditions. Then at time $t = 0$, (23) reduces to

$$(bf'')' + \frac{P+1}{2} ff'' - P(f')^2 + P_3 = x\left(f' \frac{\partial f'}{\partial x} - f'' \frac{\partial f}{\partial x}\right) \tag{27}$$

where, for example,

$$P_3 = \frac{x}{u_o^2} u_e \frac{du_e}{dx}$$

In terms of transformed variables, the eddy viscosity formulas can be written as

$$(\varepsilon_m^+)_i = 0.16 R_x^{1/2} \eta^2 \, |f''| [1 - \exp(-y/A)]^2 \tag{28a}$$

$$(\varepsilon_m^+)_o = \alpha R_x^{1/2} [f'_\infty \eta_\infty - f_\infty] \tag{28b}$$

Here the subscript refers to the boundary-layer edge and

$$R_x = \frac{u_o x}{\nu} \quad , \quad \frac{y}{A} = \frac{R_x^{1/4} (f''_w)^{1/2}}{26} \eta \, [1 - 11.8(p_t^+ + p_x^+)]^{1/2} \tag{29}$$

## III. NUMERICAL METHOD

We use a two-point finite-difference method to solve the system given by (23), (25)-(27). This method, developed by H. B. Keller[11], has been applied to two-dimensional flows by Keller and Cebeci[12], to three-dimensional flows by Cebeci[6,7]. Here we apply it to two-dimensional time-dependent flows.

We first consider (26) and write it in terms of a first-order system of partial differential equations. For this purpose we introduce new variables $u(t,\eta)$, $v(t,\eta)$ so that (26) can be written as

$$f' = u \tag{30a}$$

$$u' = v \tag{30b}$$

$$v' + P_1 fv - Pu^2 + P_3 = \frac{x}{u_o}\frac{\partial u}{\partial t} \tag{30c}$$

Here

$$P_1 = \frac{P + 1}{2} \quad ,$$

We next consider the net rectangle shown in Figure 2. We denote the net points by

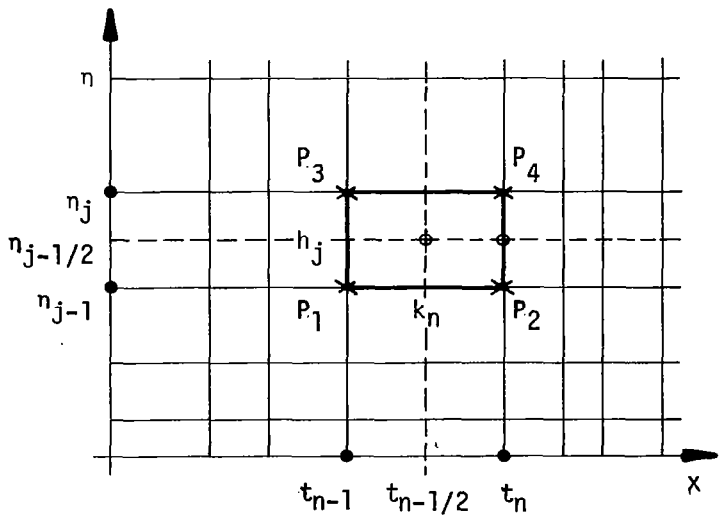


Figure 2. Net rectangle for equation (26).

$$t_0 = 0 \qquad t_n = t_{n-1} + k_n \qquad n = 1, 2, \ldots, N \tag{31a}$$

$$\eta_0 = 0 \qquad \eta_j = \eta_{j-1} + h_j \qquad j = 1, 2, \ldots, J$$
$$\eta_J = \eta_\infty \tag{31b}$$

Here the net spacings, $k_n$ and $h_j$ are completely arbitrary, and indeed may have large variations in practical calculations. The variable net spacing $h_j$ is especially important in turbulent boundary-layer calculations which are characterized by large boundary-layer thicknesses. To get accuracy near the wall, small net spacing is required while large spacing can be used away from the wall.

We approximate the quantities $(f, u, v)$ at points $(t_n, \eta_j)$ of the net by net functions denoted by $(f_j^n, u_j^n, v_j^n)$. We also employ the notation, for points and quantities midway between net points and for <u>any</u> net function $g_j^n$:

$$t_{n-1/2} = \frac{1}{2}(t_n + t_{n-1}), \quad \eta_{j-1/2} = \frac{1}{2}(\eta_j + \eta_{j-1})$$
$$g_j^{n-1/2} = \frac{1}{2}(g_j^n + g_j^{n-1}), \quad g_{j-1/2}^n = \frac{1}{2}(g_j^n + g_{j-1}^n) \tag{32}$$

The difference equations which are to approximate (30) are formulated by considering one mesh rectangle as in Figure 2. We approximate (30a,b) using centered difference quotients and average about the midpoint $(t_n, \eta_{j-1/2})$ of the segment $P_2P_4$.

$$\frac{f_j^n - f_{j-1}^n}{h_j} = u_{j-1/2}^n \tag{33a}$$

$$\frac{u_j^n - u_{j-1}^n}{h_j} = v_{j-1/2}^n \tag{33b}$$

Similarly (30c) is approximated by centering about the midpoint $t_{n-1/2}$, $\eta_{j-1/2}$ of the rectangle $P_1P_2P_3P_4$. This gives:

$$\frac{v_j^n - v_{j-1}^n}{h_j} + P_1^n(fv)_{j-1/2}^n - P^n(u^2)_{j-1/2}^n - \nu u_{j-1/2}^n = T_{j-1/2}^{n-1} \tag{33c}$$

where

$$\gamma = \frac{2x_n}{(u_o)_n k_n}$$

$$r_{j-1/2}^{n-1} = -\gamma u_{j-1/2}^{n-1} - (P_3)^{n-1/2} - \left[ \frac{v_j^{n-1} - v_{j-1}^{n-1}}{h_j} + P_1^{n-1}(fv)_{j-1/2}^{n-1} - P^{n-1}(u^2)_{j-1/2}^{n-1} \right] \tag{34}$$

The boundary conditions are:

$$f_o^n = 0, \quad u_o^n = 0, \quad u_J^n = \frac{u_e^n}{(u_o)_n} \tag{35}$$

We next consider (27) and again write it in terms of a first-order system by introducing $u(x,n)$, $v(x,n)$. This allows (27) to be written as (30a,b) and

$$(bv)' + P_1 fv - P u^2 + P_3 = x\left(u \frac{\partial u}{\partial x} - v \frac{\partial f}{\partial x}\right) \tag{36}$$

The net rectangle is the same as before, except now $t$ is replaced by $x$ and the net points in the x-direction are represented by

$$x_0 = 0, \qquad x_i = x_{i-1} + r_i, \quad i = 1, 2, \ldots I \tag{37}$$

The difference equations to (30a,b) are

$$\frac{f_j^i - f_{j-1}^i}{h_j} = u_{j-1/2}^i \tag{38a}$$

$$\frac{u_j^i - u_{j-1}^i}{h_j} = v_{j-1/2}^i \tag{38b}$$

Similarly the difference equations for (36) are:

$$\frac{(bv)_j^i - (bv)_{j-1}^i}{h_j} + (P_1^i + \alpha_i)(fv)_{j-1/2}^i - (P^i + \alpha_i)(u^2)_{j-1/2}^i + \alpha_i(v_{j-1/2}^{i-1} f_{j-1/2}^i - f_{j-1/2}^{i-1} v_{j-1/2}^i) = S_{j-1/2}^{i-1} \tag{38c}$$

Here

$$\alpha_i = \frac{x_{i-1/2}}{r_i} \tag{39a}$$

$$S_{j-1/2}^{i-1} = \alpha_i \left[ -(u^2)_{j-1/2}^{i-1} + (fv)_{j-1/2}^{i-1} \right] - (P_3)^{i-1/2} - \left[ \frac{(bv)_j^{i-1} - (bv)_{j-1}^{i-1}}{h_j} + P_1^{i-1}(fv)_{j-1/2}^{i-1} - P^{i-1}(u^2)_{j-1/2}^{i-1} \right] \tag{39b}$$

We now consider the general equation (23) and write it in terms of a system of first-order equations. We introduce variables $u(x,t,n)$, $v(x,t,n)$ so that (23) can be written as

$$f' = u \tag{40a}$$

$$u' = v \tag{40b}$$

$$(bv)' + P_1 fv - Pu^2 + P_3 = x \left( u \frac{\partial u}{\partial x} - v \frac{\partial f}{\partial x} + \frac{1}{u_0} \frac{\partial u}{\partial t} \right) \tag{40c}$$

We now consider the net cube shown in Figure 3.

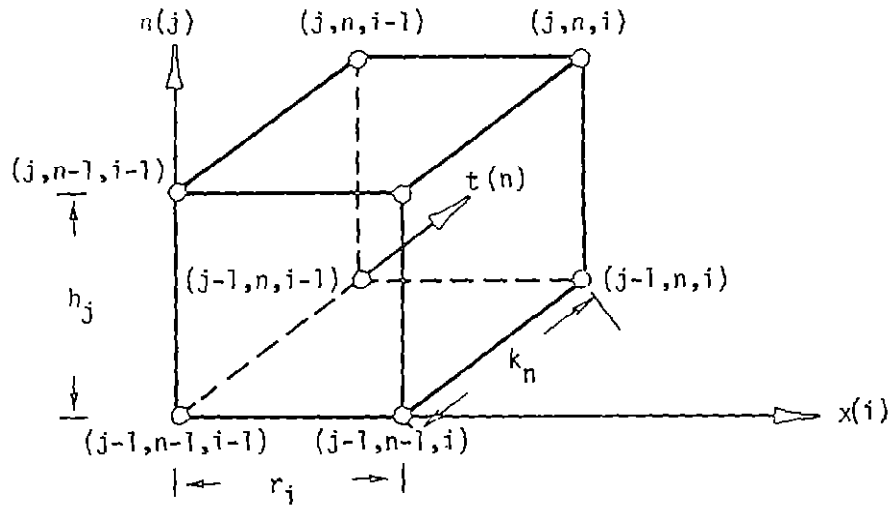


Figure 3. Net cube for the difference equations for (40).

For the net points given by (31) and (37), we approximate the quantities $(f, u, v)$ at points $(x_i, t_n, n_j)$ of the net by net function denoted by $(f_j^{i,n}, u_j^{i,n}, v_j^{i,n})$. The equations (40a,b) are approximated using centered difference quotients and averaged about the midpoint $(x_i, t_n, n_{j-1/2})$, that is

$$\frac{f_j^{i,n} - f_{j-1}^{i,n}}{h_j} = u_{j-1/2}^{i,n} \tag{41a}$$

$$\frac{u_j^{i,n} - u_{j-1}^{i,n}}{h_j} = v_{j-1/2}^{i,n} \tag{41b}$$

where, for example,

$$u_{j-1/2}^{i,n} = \frac{1}{2}\,(u_j^{i,n} + u_{j-1}^{i,n})$$

The difference equations which are to approximate (40c) are:

$$\frac{(\overline{bv})_j - (\overline{bv})_{j-1}}{h_j} + (P_1)_{n-1/2}^{i-1/2}(\overline{fv})_{j-1/2} - (P)_{n-1/2}^{i-1/2}(\overline{u^2})_{j-1/2} + (P_3)_{n-1/2}^{i-1/2}$$

$$= \frac{x^{i-1/2}}{r_i}\,[(\overline{u})_{j-1/2}(\overline{u}_i - \overline{u}_{i-1}) - \overline{v}_{j-1/2}(\overline{f}_i - \overline{f}_{i-1})]$$

$$+ \frac{x^{i-1/2}}{k_n u_o^{i-1/2}}\,(\overline{u}_n - \overline{u}_{n-1}) \tag{42}$$

where, for example,

$$\overline{v}_j = \frac{1}{4}\,(v_j^{i,n} + v_j^{i-1,n} + v_j^{i-1,n-1} + v_j^{i,n-1}) = \frac{1}{4}\,(v_j^{i,n} + v_j^{234}) \tag{43a}$$

$$\overline{u}_i = \frac{1}{4}\,(u_j^{i,n} + u_j^{i,n-1} + u_{j-1}^{i,n} + u_{j-1}^{i,n-1}) = \frac{1}{2}\,(u_{j-1/2}^{i,n} + u_{j-1/2}^{i,n-1}) \tag{43b}$$

$$\overline{u}_n = \frac{1}{4}\,(u_j^{i,n} + u_j^{i-1,n} + u_{j-1}^{i,n} + u_{j-1}^{i-1,n}) = \frac{1}{2}\,(u_{j-1/2}^{i,n} + u_{j-1/2}^{i-1,n}) \tag{43c}$$

$$(P_1)_{n-1/2}^{i-1/2} = \frac{1}{4}\,(P_n^i + P_n^{i-1} + P_{n-1}^i + P_{n-1}^{i-1}) \tag{43d}$$

Here by $v_j^{234}$ we mean $v_j^{234} = v_j^{n,i-1} + v_j^{n-1,i-1} + v_j^{n-1,i}$, the sum of the values of $v_j$ at three of the four corners of the face of the box. Introducing (43) and similar definitions for other terms into (42), after considerable algebra, we get

$$(bv)_j - (bv)_{j-1} + h_j \Big\{ (P_1)^{i-1/2}_{n-1/2}(fv)_{j-1/2} - (P)^{i-1/2}_{n-1/2}(u^2)_{j-1/2}$$
$$- \frac{\alpha_i}{2}\Big[u_{j-1/2}(u_{j-1/2} + u^{234}_{j-1/2} + u^{i,n-1}_{j-1/2} - 2\bar{u}_{i-1}) - v_{j-1/2}f_{j-1/2}$$
$$- (f^{i,n-1}_{j-1/2} - 2\bar{f}_{i-1})v_{j-1/2} - v^{234}_{j-1/2}f_{j-1/2}\Big] - 2\beta_n u_{j-1/2}\Big\} = T^{i-1,n-1}_{j-1/2} \tag{44}$$

Here

$$\beta_n = \frac{x_{i-1/2}}{k_n(u_o)^{i-1/2}} \tag{45a}$$

$$T^{i-1,n-1}_{j-1/2} = (bv)^{234}_{j-1} - (bv)^{234}_j + h_j \Big\{ -(P_1)^{i-1/2}_{n-1/2}(fv)^{234}_{j-1/2} + (P)^{i-1/2}_{n-1/2}(u^2)^{234}_{j-1/2}$$
$$- 4(P_3)^{i-1/2}_{n-1/2} + \frac{\alpha_i}{2}\Big[u^{234}_{j-1/2}(u^{i,n-1}_{j-1/2} - 2\bar{u}_{i-1}) - v^{234}_{j-1/2}(f^{i,n-1}_{j-1/2} - 2\bar{f}_{i-1})\Big]$$
$$+ 2\beta_n(u^{i-1,n}_{j-1/2} + 2\bar{u}_{n-1})\Big\} \tag{45b}$$

We note that, for simplicity, we have dropped the superscripts $i$, $n$ in the above equations.

The boundary conditions given by (25) become

$$f_o = 0\ , \qquad u_o = 0\ , \qquad u_J = \frac{u_e}{(u_o)_n} \tag{46}$$

The difference equations (33) and (38) for the initial conditions along the t-axis, and along the x-axis, respectively, together with the difference equations (41), (44), for the general case are imposed for $j = 1, 2, \ldots, J$. If we assume $(f_j^{n-1}, u_j^{n-1}, v_j^{n-1})$ for $0 \le j \le J$, and if we assume $(f_j^{i-1}, u_j^{i-1}, v_j^{i-1})$ for $0 \le j \le J$, then (33) and (38) for $1 \le j \le J$ and their boundary conditions yield an implicit nonlinear algebraic system of $3J + 3$ equations in as many unknowns $(f_j^n, u_j^n, v_j^n)$ and $(f_j^i, u_j^i, v_j^i)$. This system can be linearized by using Newton's methods and the resulting linear system

can be solved very effectively by using the block-elimination method. A brief description of the solution procedure is given below. For details, see references 11, 12 and 13.

Let us consider the system given by (33) and (35). Using Newton's method, we can write the linearized difference equations for (33) as:

$$\delta f_j - \delta f_{j-1} - \frac{h_j}{2}(\delta u_j + \delta u_{j-1}) = (r_1)_j \tag{47a}$$

$$\delta u_j - \delta u_{j-1} - \frac{h_j}{2}(\delta v_j + \delta v_{j-1}) = (r_3)_j \tag{47b}$$

$$(s_1)_j \delta v_j + (s_2)_j \delta v_j + (s_3)_j \delta f_j + (s_4)_j \delta f_{j-1} + (s_5)_j \delta u_j + (s_6)_j \delta u_{j-1} = (r_2)_j \tag{47c}$$

Here

$$(r_1)_j = f^n_{j-1} - f^n_j + h_j u^n_{j-1/2} \tag{48a}$$

$$(r_3)_j = u^n_{j-1} - u^n_j + h_j v^n_{j-1/2} \tag{48b}$$

$$(r_2)_j = T^{n-1}_{j-1/2} - [v'_{j-1/2} + p^n_1 (fv)^n_{j-1/2} - p^n (u^2)^n_{j-1/2} - \gamma u^n_{j-1/2}] \tag{48c}$$

$$(s_1)_j = \frac{1}{h_j} + \frac{p^n_1}{2} f^n_j \tag{49a}$$

$$(s_2)_j = -\frac{1}{h_j} + \frac{p^n_1}{2} f^n_{j-1} \tag{49b}$$

$$(s_3)_j = \frac{p^n_1}{2} v^n_j \tag{49c}$$

$$(s_4)_j = \frac{p^n_1}{2} v^{n-1}_j \tag{49d}$$

$$(s_5)_j = -p^n u^n_j - \frac{\gamma}{2} \tag{49e}$$

$$(s_6)_j = -p^n u^n_{j-1} - \frac{\gamma}{2} \tag{49f}$$

The boundary conditions given by (35) become

$$\delta f_0 = 0 \quad , \quad \delta u_0 = 0 \quad , \quad \delta u_J = 0 \tag{50}$$

The system (47), (50) has a block tridiagonal structure. This is not obvious and to clarify the solution we write the system in matrix-vector form. We first define the three-dimensional vectors $\underset{\sim}{\delta}_j$ and $\underset{\sim}{r}_j$ for each value of $j$ by

$$\underset{\sim}{\delta}_j = \begin{bmatrix} \delta f_j \\ \delta u_j \\ \delta v_j \end{bmatrix} \qquad 0 \le j \le J \qquad \underset{\sim}{r}_0 = \begin{bmatrix} 0 \\ 0 \\ (r_3)_0 \end{bmatrix}$$

$$\underset{\sim}{r}_j = \begin{bmatrix} (r_1)_j \\ (r_2)_j \\ (r_3)_j \end{bmatrix} \qquad 1 \le j \le J-1 \qquad \underset{\sim}{r}_J = \begin{bmatrix} (r_1)_J \\ (r_2)_J \\ 0 \end{bmatrix} \tag{51}$$

and the $3 \times 3$ matrices $A_j$, $B_j$, $C_j$ by

$$A_0 = \begin{bmatrix} 1 & 0 & 0 \\ 0 & 1 & 0 \\ 0 & -1 & -h_1/2 \end{bmatrix} \qquad A_j \equiv \begin{bmatrix} 1 & -h_j/2 & 0 \\ (s_3)_j & (s_5)_j & (s_1)_j \\ 0 & -1 & -h_{j+1}/2 \end{bmatrix} \qquad 1 \le j \le J-1$$

$$A_J \equiv \begin{bmatrix} 1 & -h_J/2 & 0 \\ (s_3)_J & (s_5)_J & (s_1)_J \\ 0 & 1 & 0 \end{bmatrix} \qquad B_j = \begin{bmatrix} -1 & -h_j/2 & 0 \\ (s_4)_j & (s_6)_j & (s_2)_j \\ 0 & 0 & 0 \end{bmatrix} \qquad 1 \le j \le J \tag{52}$$

$$C_j \equiv \begin{bmatrix} 0 & 0 & 0 \\ 0 & 0 & 0 \\ 0 & 1 & -h_{j+1}/2 \end{bmatrix} \qquad 0 \le j \le J-1$$

In terms of the above definitions, it can be shown that the system (47) and (50) can be written as

$$\mathbb{A}\underset{\sim}{\delta}_j = \underset{\sim}{r}_j \tag{53}$$

where

$$\mathbb{A} \equiv \begin{bmatrix} A_0 & C_0 & & & & & & \\ B_1 & A_1 & C_1 & & & & & \\ & \cdot & \cdot & \cdot & & & & \\ & & \cdot & \cdot & \cdot & & & \\ & & & B_j & A_j & C_j & & \\ & & & & \cdot & \cdot & \cdot & \\ & & & & & \cdot & \cdot & \cdot \\ & & & & & & B_{J-1} & A_{J-1} & C_{J-1} \\ & & & & & & & B_J & A_J \end{bmatrix} \tag{54a}$$

$$\underset{\sim}{\delta}_j \equiv \begin{bmatrix} \underset{\sim}{\delta}_0 \\ \underset{\sim}{\delta}_1 \\ \underset{\sim}{\delta}_2 \\ \cdot \\ \cdot \\ \cdot \\ \cdot \\ \underset{\sim}{\delta}_{J-1} \\ \underset{\sim}{\delta}_J \end{bmatrix} \qquad \underset{\sim}{r}_j = \begin{bmatrix} \underset{\sim}{r}_0 \\ \underset{\sim}{r}_1 \\ \underset{\sim}{r}_2 \\ \cdot \\ \cdot \\ \cdot \\ \cdot \\ \underset{\sim}{r}_{J-1} \\ \underset{\sim}{r}_J \end{bmatrix} \tag{54b}$$

The solution of (53) is obtained by the procedure described in reference 13.

Similarly, for the general case, if we assume $(f_j^{n-1,i-1}, u_j^{n-1,i-1}, v_j^{n-1,i-1})$, $(f_j^{n,i-1}, u_j^{n,i-1}, v_j^{n,i-1})$ and $(f_j^{n-1,i}, u_j^{n-1,i}, v_j^{n-1,i})$ to be known for $0 \leq j \leq J$, then the differenced equations for the general case can be solved by a similar procedure used for the two equations for the initial conditions.

## IV. RESULTS

The present method is applicable to both laminar and turbulent boundary layers. The flow is laminar at the leading edge, and it becomes turbulent at any specified $x > 0$. The initial conditions along the $(\eta,t)$ plane are generated by solving the system given by (30) and (35), and the initial conditions along the $(\eta,x)$ plane are generated by solving the steady-flow equations, that is, (27) subject to (25).

The marching procedure is along the t-direction. For a specified x-location, the governing equations are solved for each specified t-station. Since the linearized form of the equations are being solved, we iterate at each t-station until some convergence criterion is satisfied. For both laminar and turbulent flows we use the wall-shear parameter $f''_w$ as the convergence criterion. Calculations are stopped when

$$|\delta f''_w| < \delta_1 \tag{55}$$

where the value of $\delta_1$ is prescribed.

### 4.1 Laminar Flows

There are several problems in which it is necessary to account for the fluctuations in the external flow. These fluctuations may change both in direction and in magnitude. A simpler case is one in which the external flow fluctuates only in magnitude and not in direction. This problem has been studied by Lighthill[14] for a flat-plate flow. According to his analysis, for an external flow in the form

$$u_e(t) = u_o(1 + B \cos \omega t) \tag{56}$$

the reduced skin-friction coefficient $c_f/2\sqrt{R_x}$ is given by two separate formulas depending on whether the reduced frequency $\omega x/u_o$ is much smaller or much greater than one,

$$\frac{c_f}{2}\sqrt{R_x} = \begin{cases} 0.332 + B(0.498 \cos \omega t - 0.849\, \omega x/u_o \sin \omega t), & \omega x/u_o \ll 1 \quad (57a) \\ 0.332 + B(\omega x/u_o)^{1/2} \cos(\omega t + \pi/4), & \omega x/u_o \gg 1 \quad (57b) \end{cases}$$

In many problems it is often desirable to find the phase angle between the external flow and say the reduced skin-friction coefficient, which in terms of the transformed variables defined by (20) and (21), is $f''_w$. To determine this numerically for a fixed $x = x_o$, let us consider the general case in which the external flow is given by

$$u_e(x,t) = u_o(x)(1 + B \cos \omega t) \tag{58}$$

and let

$$f''_w(x,t) = g(x,t) \tag{59}$$

We use the following procedure to determine the phase angle between $u_e(x_o,t)$ and $g(x_o,t)$. We first compute $u_o(x_o)$ and $\bar{g}(x_o)$ from

$$u_o(x_o) = \frac{1}{P} \int_{t_o}^{t_o+P} u_e(x_o,t)dt \tag{60a}$$

$$\bar{g}(x_o) = \frac{1}{P} \int_{t_o}^{t_o+P} g(x_o,t)dt \tag{60b}$$

where $P = 2\pi/\omega$ and is the period of oscillation of the maintstream. Strictly $u_o$ and $\bar{g}_o$ are functions of $t_o$ as well as of $x_o$, but for $B \leq 0.150$, it was found that transient and other effects have virtually disappeared when $t_o = P$ and this value of $t_o$ was chosen to compute them.

From (58), we can write

$$u_e(x_o,t) - u_o(x_o) = A \cos \omega t \tag{61}$$

where $A \equiv u_o(x_o)B$.

Similarly, we can write

$$g(x_o,t) - \bar{g}(x_o) = C \cos [\omega t + \phi(x_o)] = C [\cos \omega t \cos \phi(x_o) - \sin \omega t \sin \phi(x_o)] \tag{62}$$

with $\phi(x_o)$ denoting the phase angle between $u_e$ and $g$ at $x = x_o$. If we take the product of (61) and (62) and integrate the resulting expression, we find $\cos \phi(x_o)$ to be given by

$$\cos \phi(x_o) = \frac{\int_{t_o}^{t_o+P} \left\{[u_e(x_o,t) - u_o(x_o)] \cdot [g(x_o,t) - \bar{g}(x_o)]\right\} dt}{AC\ \pi/\omega} \tag{63}$$

Here

$$A^2 = \frac{\omega}{\pi} \int_{t_o}^{t_o+P} [u_e(x_o,t) - u_o(x_o)]^2 dt \tag{64a}$$

$$C^2 = \frac{\omega}{\pi} \int_{t_o}^{t_o+P} [g(x_o,t) - \bar{g}(x_o)]^2 dt \tag{64b}$$

Figure 4 shows the computed phase angle (between wall shear and external velocity) variation with reduced frequency $\omega x/u_o$ for a laminar flat-plate flow. These calculations were made for an external flow given by (56) with $B = 0.150$, $u_o = 17.5$. A total of 41 t-stations, and 26 x-stations with $\Delta t = 0.20$ and $\Delta x = 0.1$ were taken. Initially $\eta_\infty$ was taken as 8 with $\Delta\eta = 0.28$. During the calculations $\eta_\infty$ was allowed to grow. Our results (not shown in the figure) indicate that it is desirable to compute for two periods in order to determine the phase angle accurately. Figure 2 also shows the results obtained by Lighthill[14] with low frequency and high frequency approximations. These numerical calculations are in good agreement with those computed by Ackerberg and Phillips[15]; they show that if $\tilde{B} \leq 0.150$, Lighthill's low-frequency approximations to the phase angle are accurate for $\omega \leq 0.2u_o/x$ and his high frequency approximation is accurate for $\omega \geq 2.6u_o/x$.

If we write the wall shear as

$$\tau = \tau_o + \tilde{B}\tau_1 \cos(\omega t + \phi),$$

then it follows that

$$\frac{\tau_1}{\tau_o} = \frac{(\tau/\tau_o - 1)}{\tilde{B} \cos(\omega t + \phi)} \tag{65}$$

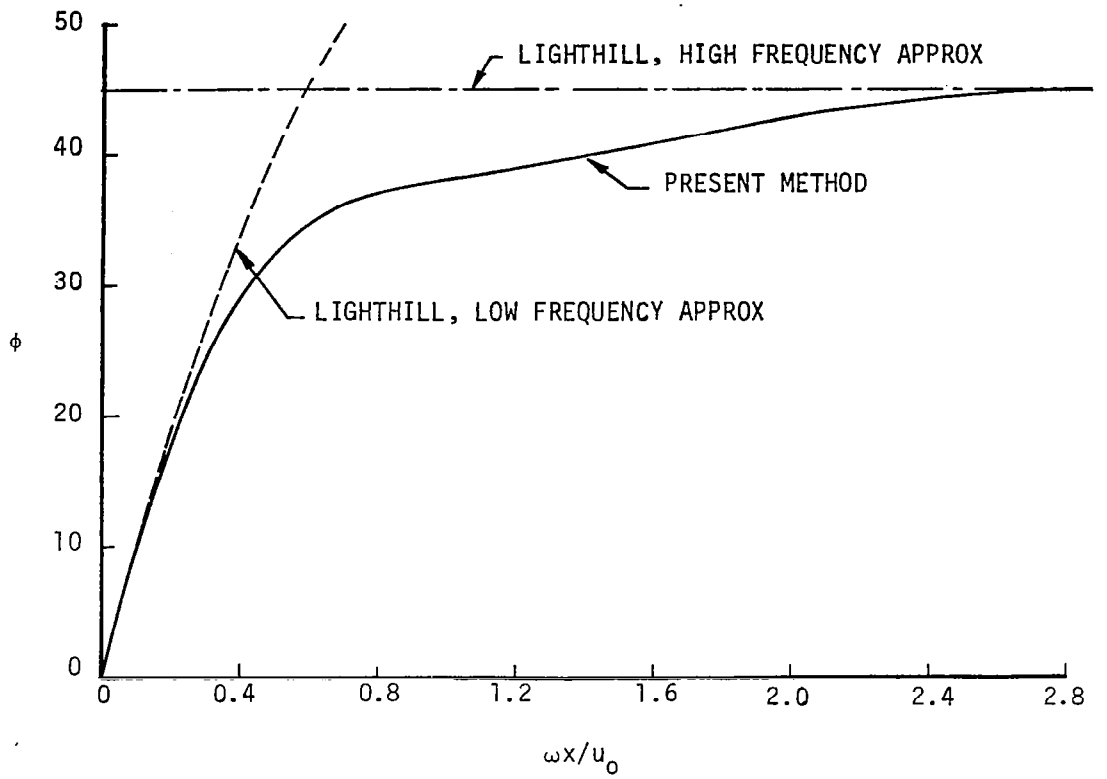


Figure 4. Variation of phase angle between wall shear and oscillating external velocity for a laminar flow over a flat plate.

where $\tau_0$ is the wall shear for Blasius flow, then again $\tau_1$ is strictly a function of x, B and t. However, with $\phi$ defined by (63) it appears that $\tau_1$ in independent of B and the t-dependence has virtually disappeared when $t > P$ in the calculations. It, thus, appears that nonlinear effects are negligible for $B \leq 0.150$. In terms of our transformed variables ,

$$\frac{\tau_1}{\tau_0} = \frac{f''_w(x,t) - (f''_w)_{f.p.}}{(f''_w)_{f.p.}\, B \cos(\omega t + \phi)} \tag{66}$$

and Figure 5 shows the computed values of $\tau_1/\tau_0$ for $t = 2P$ together with Lighthill's low frequency and high frequency approximations. The agreement is good, the error at large $\omega x/u_0$ being approximately equal to $B$ in magnitude.

## 4.2 Turbulent Flows

The experimental data on unsteady turbulent boundary layers is very limited. The only data known to the author is that of Karlsson[16], which consists of an

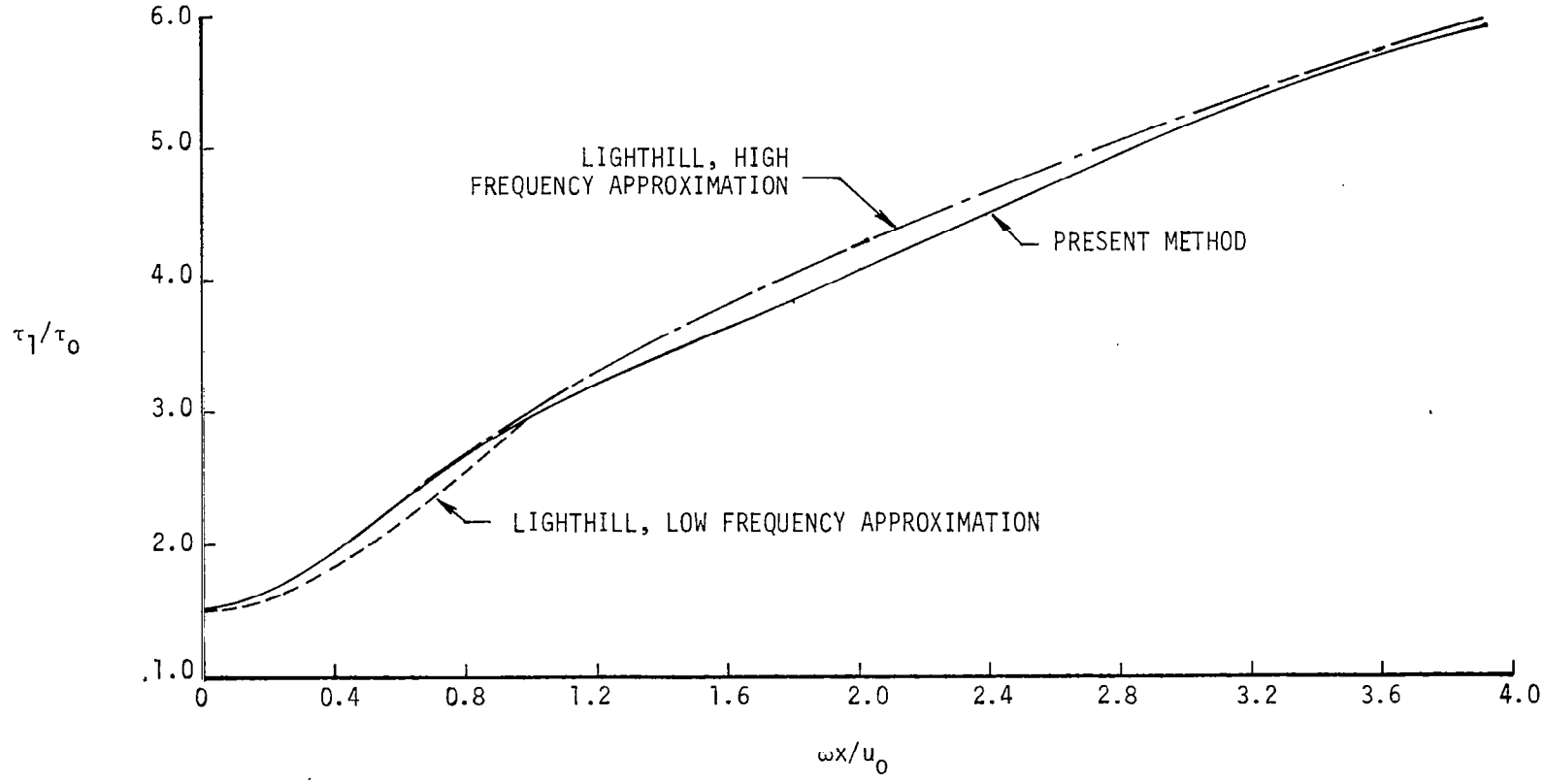


Figure 5. Variation of amplitude of the wall shear fluctuations for an oscillating laminar flow over a flat plate.

oscillating free stream in a zero pressure gradient turbulent flow. The measurements were made for a Reynolds number of $R_{\delta^*}(\equiv u_o\delta^*/\nu) = 3.6 \times 10^3$. Here

$$\delta^* = \int_0^\infty \left(1 - \frac{u}{u_o}\right) dy$$

In order to compare our numerical calculations with this data, we take the external flow to be the same as (56) and for convenience write it as

$$u_e = u_o + u_o\tilde{B} \cos \omega t \tag{67}$$

Here $u_o\tilde{B} = u_\infty^{(1)}$ according to Karlsson's notation.

We follow Karlsson's notation and denote the x-component of the velocity within the boundary layer by

$$u(x,y,t) = \bar{u}(x,y) + u^{(1)} \cos \phi \cos \omega t - u^{(1)} \sin \phi \sin \omega t \tag{68}$$

But since $f' = u/u_o$, we can write the above expression as

$$u_o f' = \bar{u}(x,y) + u^{(1)} \cos \phi \cos \omega t - u^{(1)} \sin \phi \sin \omega t \tag{69}$$

Using (67), we write (69) as

$$\frac{u}{u_\infty^{(1)}} = \frac{f'}{\tilde{B}} = \frac{\bar{u}}{u_o\tilde{B}} + \frac{u^{(1)} \cos \phi}{u_\infty^{(1)}} \cos \omega t - \frac{u^{(1)} \sin \phi}{u_\infty^{(1)}} \sin \omega t \tag{70}$$

Karlsson gives $\bar{u}/u_o$, $u^{(1)} \cos \phi/u_\infty^{(1)}$ and $u^{(1)} \sin \phi/u_\infty^{(1)}$ for different frequencies $(\omega/2\pi)$ and for different free-stream amplitudes $\tilde{B}$. To compute $u^{(1)} \cos \phi/u_\infty^{(1)}$ from (70) we multiply both sides by $\cos \omega t$ and integrate with respect to $t$ from 0 to $2\omega/\pi$ to get

$$A(\eta) \equiv \frac{u^{(1)} \cos \phi}{u_\infty^{(1)}} = \frac{\omega}{\pi} \frac{1}{\tilde{B}} \int_0^{2\pi/\omega} f'(\eta,t) \cos \omega t dt \tag{71}$$

Similarly, to get $u^{(1)} \sin \phi/u_\infty^{(1)}$, we multiply both sides by $\sin \omega t$ and integrate. That gives,

$$B(\eta) \equiv \frac{u^{(1)}}{u_\infty^{(1)}} \sin\theta = -\frac{\omega}{\pi}\frac{1}{\tilde{B}}\int_0^{2\pi/\omega} f'(\eta,t)\sin\omega t\,dt \tag{72}$$

To compute $A(\eta)$ and $B(\eta)$ we take uniform steps in $\Delta t$ and noting that

$$\Delta t = \frac{2\pi}{\omega N} \quad , \qquad t = n\Delta t_n \quad , \qquad n = 1, 2, \ldots, N \tag{73}$$

we approximate (71) and (72) by [recalling $(f')_j^n = f'(\eta_j, t_n)$]

$$A_j = \frac{2}{\tilde{B}N}\sum_{n=0}^{N}(f'_j)^n \cos\omega t_n \tag{74}$$

$$B_j = -\frac{2}{\tilde{B}N}\sum_{n=0}^{N}(f'_j)^n \sin\omega t_n \tag{75}$$

Figures 6 to 8 show the results for Karlsson's data. These calculations were started as laminar at $x = 0$ for the external flow given by (67) with

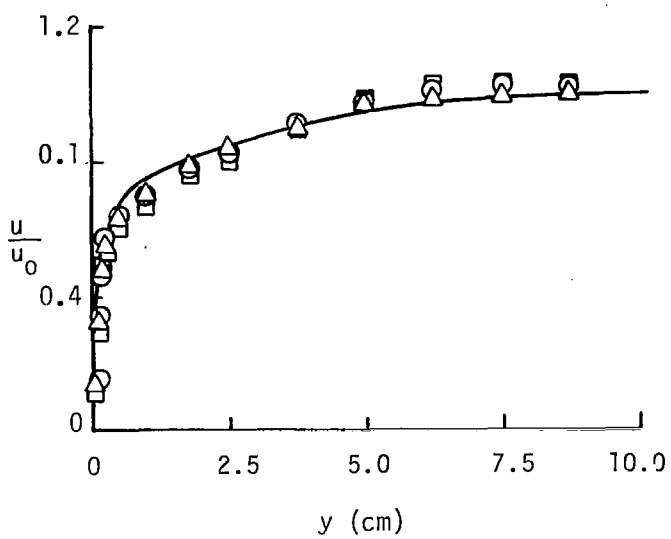


Figure 6. Comparison of calculated and experimental velocity profiles at $R_{\delta^*} \equiv 3.6 \times 10^3$. Symbols denote $u/u_0$ for values of $\tilde{B} = 0.292$, 0.202 and 0.147.

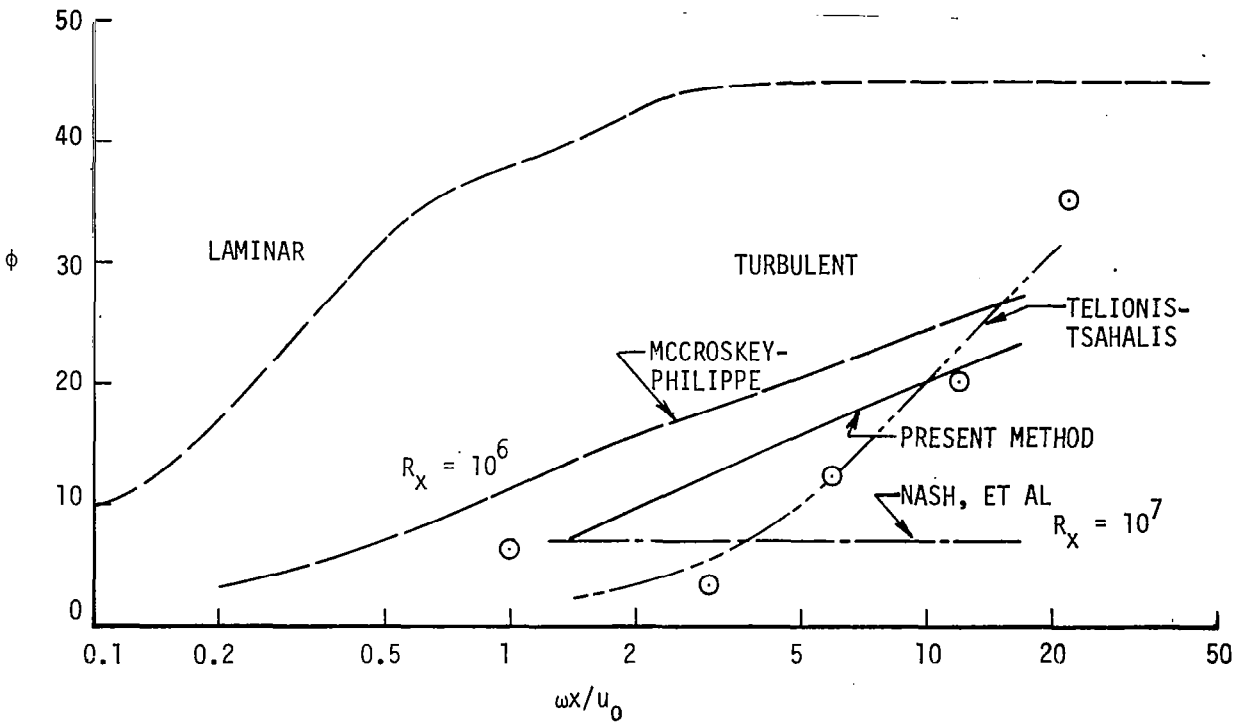


Figure 7. Variation of phase angle between wall shear and oscillating external velocity for laminar and turbulent flows over a flat plate. The symbols denote Telionis' interpretation of Karlsson's data.

(a)

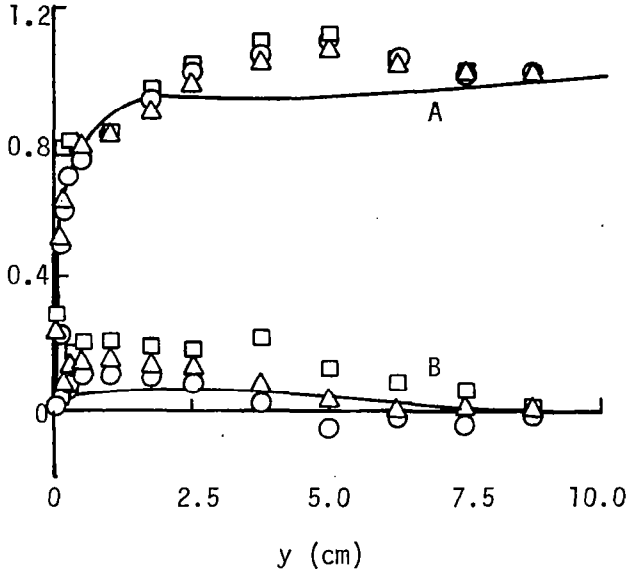


Figure 8. Comparison of calculated and experimental values of the in-phase (A) and out-of-phase (B) components of an oscillating turbulent flow over a flat plate. (a) Experimental data are for $\omega/2\pi$ = 0.33 cycles/sec; $u_\infty^{(1)}/u_0$ = 29.2% (o), 20.2% (Δ), 14.7% (□). Calculations for for $u_\infty^{(1)}/u_0$ = 14.7%

(b)

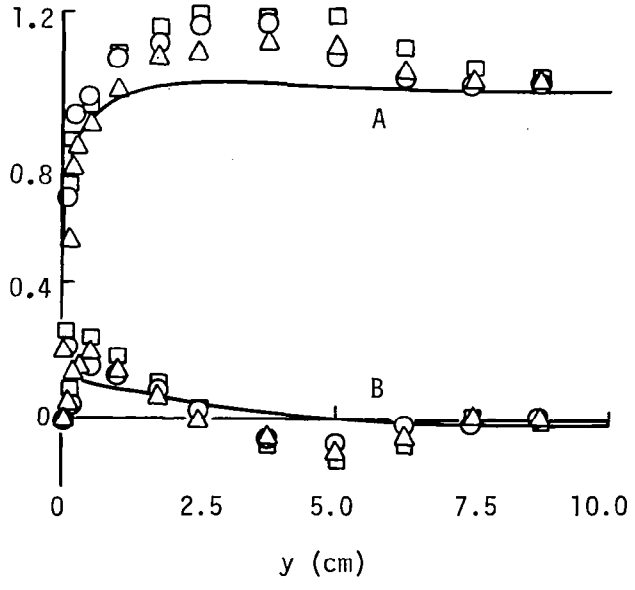


Figure 8. (b) Experimental data are for $\omega/2\pi$ = 1.0 cycles/sec; $u_\infty^{(1)}/u_0$ = 35.2% (o), 19.5%(Δ), 10.7% (□). Calculations are for $u_\infty^{(1)}/u_0$ = 35.2%.

(c)

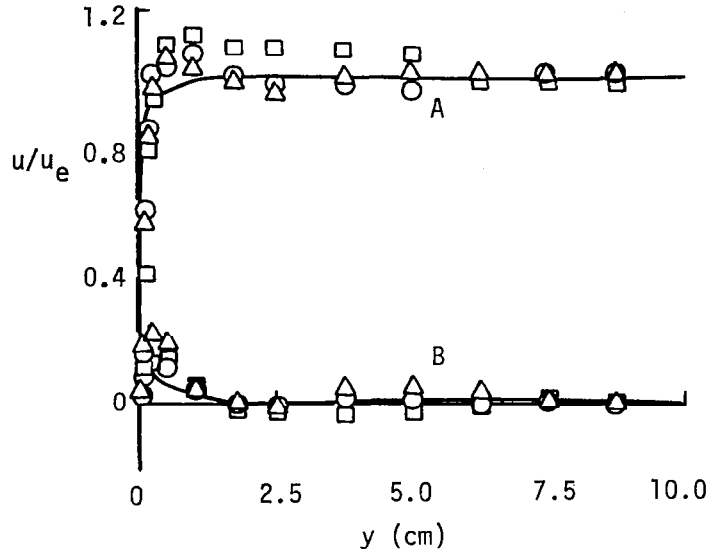


Figure 8. (c) Experimental data are for $\omega/2\pi$ = 4.0 cycles/sec; $u_\infty^{(1)}/u_0$ = 26.4% (○), 13.6% (△), 6.2% (□). Calculations are for $u_\infty^{(1)}/u_0$ = 26.4%.

$u_0$ = 5.33 m/sec. The $\Delta x$-spacing for turbulent flows was one foot. The turbulent flow calculations were started at $x$ = 3.05 cm, and at $z \approx 3.7$ m the experimental velocity profile was matched (see figure 6). We note that the experimental velocity profile is essentially unchanged for various magnitudes (small) of external flow.

Figure 7 shows the variation of phase angle (between wall shear and edge velocity) with reduced frequency $\omega x/u_0$ for laminar and turbulent flows. The results indicated by the present method were obtained by the procedure discussed above for $\omega/2\pi$ = 0.33, 1, 4 cycles/sec with $\tilde{B}$ = 0.147, 0.352 and 0.264, respectively. The other results shown in this figure are obtained from a figure given by McCroskey[17]. In that figure, McCroskey gives a comparison between numerical studies by McCroskey and Philippe, Telionis and Tsahalis, and Nash et al., and also some experimental data due to Karlsson interpreted by Telionis. The phase angle distribution for laminar flows is computed by the present method and is included for comparison purposes.

Figure 8 shows the comparison between calculated and experimental values of the in-phase and out-of-phase components, that is, $u^{(1)} \cos \phi/u_\infty^{(1)}$ and $u^{(1)} \sin \phi/u_\infty^{(1)}$, respectively, for the three different frequencies and amplitudes mentioned earlier. It is interesting to note that of these three cases,

only the $u^{(1)}\sin\phi/u_\infty^{(1)}$ – distribution corresponding to $\omega/2\pi = 1$ has positive and negative values, just like the computed ones!

Table 1 presents the ratio $\tau_1/\tau_0$ for laminar and turbulent flows. It can be shown that $\tau_1/\tau_0$ can be calculated from

$$\frac{\tau_1}{\tau_0} = \frac{c_f/c_{f_0} - 1}{\tilde{B}\cos(\omega t + \phi)} \tag{76}$$

Here $c_{f_0}$ denotes the flat-plate skin friction; it can be calculated from the following formula given by Cebeci and Smith[5]

$$c_{f_0} = \frac{2}{(2.44 \ln R_{\delta^*} + 4.43)^2} \tag{77}$$

The results shown in Table 1 indicate that in turbulent flows the ratio $\tau_1/\tau_0$ is much smaller than its value in laminar flows. We also observe that for turbulent flows the variation of $\tau_1/\tau_0$ with reduced frequency is relatively small compared to its variation for laminar flows; this is consistent with the results reported by McCroskey and Philippe[1].

Table 1. Variation of $\tau_1/\tau_0$ with Reduced Frequency, $\tilde{\omega}$

| | $\tau_1/\tau_0$ | |
|---|---|---|
| $\tilde{\omega}$ | Laminar | Turbulent |
| 1.36 | 3.3 | 2.28 |
| 1.48 | 3.50 | 2.39 |
| 4.50 | 6.50 | 2.75 |

## V. CONCLUDING REMARKS

A numerical method for computing two-dimensional incompressible unsteady laminar and turbulent boundary layers with fluctuations in external velocity is presented. The Reynolds shear stress term is modeled by using the algebraic eddy-viscosity formulas developed by the author. The numerical accuracy of the method is first checked for laminar flows and the results are compared by Lighthill's analytical solutions as well as by those obtained by other numerical methods. Based on these comparisons it is found that the method is quite accurate.

Similar calculations are also made for turbulent flows and the results are compared with available experimental data and with other numerical solutions. In general the present results agree reasonably well with experimental data and with those obtained by other numerical methods, McCroskey and Philippe[1] and Telionis[2], which also used the present author's eddy-viscosity formulation, Cebeci[5]. The present eddy-viscosity formulation is slightly different than that reported in Cebeci[5] in that it allows the unsteady effects through $p_t^+$ in equation (18). Furthermore, it also accounts for the low Reynolds number effect which was not included in Telionis' calculations[2]. Another difference between the present results and with those obtained by McCroskey and Philippe and Telionis and Tashalis may be due to the procedure used in computing phase angles and the procedure used to generate the initial conditions required to make the turbulent flow calculations.

Although our turbulent flow calculations agree reasonably well with Karlsson's experimental data and with those methods that use algebraic eddy-viscosity formulas, they do not agree with those computed by Nash et al. This is somewhat surprising because that method is a modified version of Bradshaw's method, and that the predictions of this method for steady flows, see ref. (5), and unsteady flows, see ref. (10), agreed well with the predictions of the author's method.

## VI. REFERENCES


1. McCroskey, W.J. and Philippe, J.J.: Unsteady Viscous Flow on Oscillating Airfoils, AIAA J., 13, p. 71-79, 1975.

2. Telionis, D.P.: Calculation of Time-Dependent Boundary Layers, in Unsteady Aerodynamics, Vol. 1, R. B. Kinney (Ed.), The University of Arizona, p. 155-190, 1975.

3. Nash, J.F., Carr, L.W., and Singleton, R.: Unsteady Turbulent Boundary Layers in Two-Dimensional Incompressible Flow, AIAA J., 13, p. 167-172, 1975.

4. Patel, V.C. and Nash, J.F.: Unsteady Turbulent Boundary Layers with Flow Reversal, in Unsteady Aerodynamics, Vol. 1, R. B. Kinney (Ed.), The University of Arizona, p. 191-220, 1975.

5. Cebeci, T. and Smith, A.M.O.: Analysis of Turbulent Boundary Layers. Academic Press, New York, 1974.

6. Cebeci, T.: Calculation of Three-Dimensional Boundary Layers. I. Swept Infinite Cylinders and Small Cross-Flow, AIAA J., 12, p. 779-786, 1974.

7. Cebeci, T.: Calculation of Three-Dimensional Turbulent Boundary Layers, II. Three-Dimensional Flows in Cartesian Coordinates, AIAA J., 13, p. 1056-1064, 1975.

8. Back, L.H., Cuffel, R.F. and Massier, P.F.: Laminarization of a Turbulent Boundary Layer in Nozzle Flow — Boundary Layer and Heat Transfer Measurements with Wall Cooling, J. Heat Transfer, Ser. C, 92, p. 333, 1970.

9. Einstein, H.A. and Li, H.: The Viscous Sublayer Along a Smooth Boundary. Am. Soc. Civil Eng., 123, p. 293-317, 1958.

10. Cebeci, T. and Keller, H.B.: On the Computation of Unsteady Turbulent Boundary Layers, in Recent Research on Unsteady Boundary Layers, E. A. Eichelbrenner (Ed.), II, p. 1072-1105, 1972.

11. Keller, H.B.: A New Difference Scheme for Parabolic Problems,in Numerical Solution of Partial Differential Equations, J. Bramble (Ed.), II, Academic Press, New York, 1970.

12. Keller, H.B. and Cebeci, T.: Accurate Numerical Methods for Boundary Layers. II. Two-Dimensional Turbulent Flows, AIAA J., 10, p. 1197-1200, 1972.

13. Cebeci, T. and Bradshaw, P.: Momentum Transfer in Boundary Layers, McGraw-Hill/Hemisphere, Washington, D.C., 1977.

14. Lighthill, M.J.: The Response of Laminar Skin Friction and Heat Transfer to Fluctuations in the Stream Velocity. Proc. Roy. Soc., 224A, p. 1-23, 1954.

15. Ackerberg, R.C. and Phillips, J.H.: The Unsteady Laminar Boundary Layer on a Semi-Infinite Flat Plate Due to Small Fluctuations in the Magnitude of the Free-Stream Velocity. J. Fluid Mech., Vol. 51, p. 137-157, 1972.

16. Karlsson, S.K.F.: An Unsteady Turbulent Boundary Layer. J. Fluid Mech., 5, p. 622-636, 1959.

17. McCroskey, W.J.: Some Current Research in Unsteady Aerodynamics — A Report From the Fluid Dynamics Panel. Presented at 46th Meeting of AGARD Propulsion and Energetics Panel, Monterey, Calif., 1975.